Journal of The Electrochemical Society, **155** (3) J66-J70 (2008)
0013-4651/2008/155(3)/J66/5/$23.00 © The Electrochemical Society

Effects of Eu^{2+} Concentration Variation and Ce^{3+} Codoping on Photoluminescence Properties of $BaGa_2S_4:Eu^{2+}$ Phosphor

Hyoung Sun Yoo, Won Bin Im, Sivakumar Vaidyanathan, Bong Je Park, and Duk Young Jeon*,z

Department of Materials Science and Engineering, Korea Advanced Institute of Science and Technology, Daejeon 305-701, Korea

$Ba_{1-x-2y}Eu_xCe_yLi_yGa_2S_4$ phosphor samples were synthesized by a solid-state reaction method. The lattice parameter of the $Ba_{1-x}Eu_xGa_2S_4$ phosphor samples was linearly decreased from 12.654 to 12.492 Å, and the main emission wavelength was shifted from 501 to 530 nm with increase of the Eu^{2+} ion concentration (x) from 0.05 to 0.50. The relative photoluminescence (PL) intensity under 450 nm excitation was increased with increase of the x from 0.05 to 0.25 due to the excitation band extended to the longer wavelength. However, when $x > 0.30$, the PL intensity was decreased due to nonradiative transitions among the Eu^{2+} ions and the formation of $EuGa_2S_4$ impurity phase. The Commission International de l'Eclairge chromaticity coordinates were also largely shifted from the bluish-green emitting region ($x = 0.143$, $y = 0.506$) to the green emitting one ($x = 2.414$, $y = 0.658$) by increasing the x from 0.05 to 0.50. The energy transfer from the Ce^{3+} ion to the Eu^{2+} ion enhanced the PL intensity of the Eu^{2+} ion emission under near ultraviolet and blue excitation. The PL intensity of the $Ba_{0.900}Eu_{0.050}Ce_{0.025}Li_{0.025}Ga_2S_4$ phosphor sample was higher by 24% than that of the $Ba_{0.95}Eu_{0.05}Ga_2S_4$ phosphor sample under 450 nm excitation.
 [DOI: 10.1149/1.2825303]

Manuscript submitted October 1, 2007; revised manuscript received November 12, 2007. Available electronically January 7, 2008.

Recently, white light-emitting diodes (LEDs) have been widely investigated for backlight units of liquid crystal displays, flashlights, decorative illuminations, and general lighting applications due to their promising features, such as high energy efficiency, good reliability, long lifetime, mercury-free, and small size. Many investigations have been carried out to improve the luminous efficiency and the color-rendering properties of the white LEDs for expanding their market size. The first white LEDs were fabricated by a combination of InGaN-based blue LEDs and yellow phosphors, such as $(Y, Tb)_3(Al, Ga)_5O_{12}:Ce^{3+}$,[1] $Sr_2SiO_4:Eu^{2+}$,[2] $Li_2SrSiO_4:Eu^{2+}$,[3] Ca-α-SiAlON:Eu^{2+}[4] and $(Ca, Sr)Si_2O_{2-\delta}N_{2+2/3\delta}:Eu^{2+}$ phosphors.[5] These two band white LEDs generally showed the color-rendering index (CRI) value of <80, but it was not high enough yet for general lightings and medical applications. Thereafter, in order to increase the CRI values of white LEDs, three band white LEDs mixed with blue LEDs and red/green emitting phosphors or four band white LEDs with red/yellow/green emitting phosphors have been investigated. Both nitride phosphors, such as β-SiAlON:Eu^{2+},[6] $CaAlSiN_3:Eu^{2+}$,[7] and $Sr_2Si_5N_8:Eu^{2+}$,[8] and sulfide phosphors, such as $SrGa_2S_4:Eu^{2+}$, ZnCdS:Ag^+, Cl^-,[9] (Ca, Sr)S:Eu^{2+} were adopted as the red/green phosphors. Recently, Kimura et al. fabricated the white LEDs with extremely high CRI values of 95–98 and the luminous efficacies of 28–35 lm/W by adopting $BaSi_2O_2N_2:Eu^{2+}$ bluish-green emitting phosphor.[10] It is expected that the high color-rendering white LEDs combined with a bluish-green emitting phosphor will be widely used in many applications.

The $BaGa_2S_4:Eu^{2+}$ phosphor is one of many bluish-green emitting phosphors, which has broad absorption bands ranging from 300 to 470 nm and the main emission wavelength at ~500 nm.[11-13] Therefore, it is possible that the phosphor is applied to the white LEDs with an extra-high CRI value. In this study, we have prepared the $BaGa_2S_4:Eu^{2+}$ phosphor and investigated the photoluminescence (PL) properties depending on the Eu^{2+} ion concentrations in detail. In addition, the effects of the Ce^{3+} ion codoping on the PL properties of the phosphor were investigated.

Experimental

Synthesis.— BaS (Kojundo, 99.9%), Ga_2S_3 (Kojundo, 99.9%), Eu_2O_3 (Aldrich, 99.99%), CeO_2 (Aldrich, 99.99%), Li_2CO_3 (Aldrich 99.99%), and stoichiometric amounts of S (Aldrich, 99%) were used as raw materials to prepare the $Ba_{1-x-2y}Eu_xCe_yLi_yGa_2S_4$ ($0 \le x \le 0.500$, $0 \le y \le 0.035$) phosphor samples. For the samples with codoping of Ce^{3+} ions, Li^+ ions were also used for charge compensation. In the previous studies, an H_2S stream had been used to prevent oxidization during synthesis of the $BaGa_2S_4:Eu^{2+}$ phosphor.[11-13] However, the H_2S gas is expensive and very toxic, and thus it causes serious environmental pollutions.[9] Therefore, we synthesized the phosphor samples by using an activated carbon powder in a double-crucible configuration without allowing any atmospheric gases.[9] After mixing of raw materials in an agate mortar, the mixture was placed in a small-sized crucible. Then, the crucible was placed in a larger crucible with an activated carbon powder in between.[9] All the phosphor samples were fired at 900°C, which was the optimized temperature in terms of their crystallinity and PL properties.

Characterization.— The morphology and size of the prepared phosphor particles were observed by a Philips XL30SFEG scanning electron microscope (SEM). Crystalline phases of the phosphor samples were analyzed by a Rigaku D/max–RC X-ray diffractometer with Cu Kα ($\lambda = 1.542$ Å) radiation operating at 40 kV and 45 mA. The scan rate was 1°/min, and the measurement range was from 20 to 60°. The PL emission and excitation spectra of the prepared samples were obtained by using a Perkin-Elmer LS-50 spectrometer with a xenon flash lamp.

Results and Discussion

Phase formation.— Figure 1 shows the SEM image of the $Ba_{0.95}Eu_{0.05}Ga_2S_4$ phosphor sample. Its particles were well dispersed, and their mean size was <10 μm. Its particle shape and size distribution were not affected by the Eu^{2+} ion concentration and the codoping of Ce^{3+} ion. Figure 2 shows the X-ray diffraction (XRD) patterns of the $Ba_{1-x}Eu_xGa_2S_4$ phosphor samples prepared with various Eu^{2+} ion concentrations. The XRD pattern of the $Ba_{0.95}Eu_{0.05}Ga_2S_4$ phosphor sample was well matched with that of the cubic $BaGa_2S_4$ phase (PDF no. 76-1053, the space group Th^6–$Pa3$) without any impurity peak.[11,12] As the concentration of Eu^{2+} ion was increased, positions of the peaks in the XRD patterns shifted to larger 2θ. The shift of the peak positions to larger 2θ meant decrease of the lattice parameter and shrinkage of the unit cell. Figure 3 shows the lattice parameters of the $Ba_{1-x}Eu_xGa_2S_4$ phosphor samples, depending on the Eu^{2+} ion concentration. The lattice parameter of the $Ba_{0.95}Eu_{0.05}Ga_2S_4$ phosphor sample was the 12.654 Å, which was well matched with the results reported by Peters and Baglio.[11] Because the ionic radius of Eu^{2+} ion (1.17 Å for six coordination) is smaller than that of the Ba^{2+} ion (1.35 Å for

* Electrochemical Society Active Member.
z E-mail: dyj@kaist.ac.kr

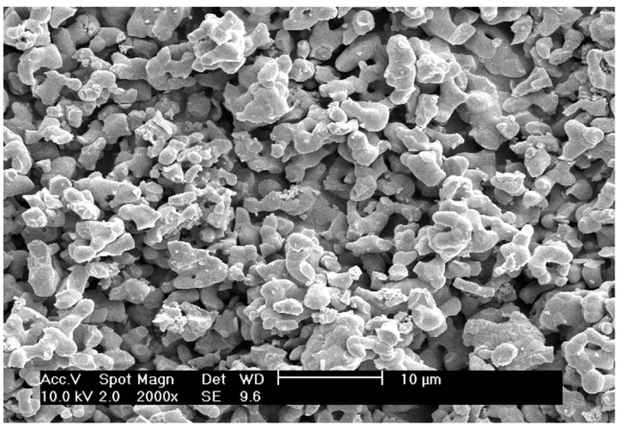

Figure 1. SEM image of the $Ba_{0.95}Eu_{0.05}Ga_2S_4$ phosphor sample.

six coordination), the lattice parameters were decreased from 12.654 to 12.492 Å with increase of the Eu^{2+} ion concentration (x) from 0.05 to 0.50. Linear decrease of the lattice parameter meant that the Eu^{2+} ions were well substituted for the Ba^{2+} ions. However, $EuGa_2S_4$ impurity phase was observed in the phosphor samples with the Eu^{2+} ion concentration (x) above 0.40. The $EuGa_2S_4$ phase has the orthorhombic structure, which is different from the cubic-based $BaGa_2S_4$ phase, and Eu^{2+} ions could not fully substitute for Ba^{2+} ions with maintaining the cubic structure due to the difference between the ionic radii. Only a small amount ($y \leq 0.035$) of Ce^{3+} ion codoping almost did not affect the lattice parameter of the $Ba_{1-x-2y}Eu_xCe_yLi_yGa_2S_4$ phosphor samples.

The PL properties of $Ba_{1-x}Eu_xGa_2S_4$.— Figure 4 shows the normalized PL spectra of the $Ba_{1-x}Eu_xGa_2S_4$ phosphor samples with various Eu^{2+} ion concentrations. For all prepared samples, the broad emission band due to the dipole-allowed transition from the $4f^6(^7F)5d$ state to the $4f^7(^8S_{7/2})$ ground state of Eu^{2+} ion was observed. The main emission wavelength of the phosphor samples was increased from 501 to 530 nm with an increase of the Eu^{2+} ion concentration (x) from 0.05 to 0.50. The normalized PL excitation (PLE) spectra of the prepared samples were shown in the inset of the Fig. 4. The PLE spectrum of the $BaGa_2S_4$:Eu^{2+} phosphor consisted

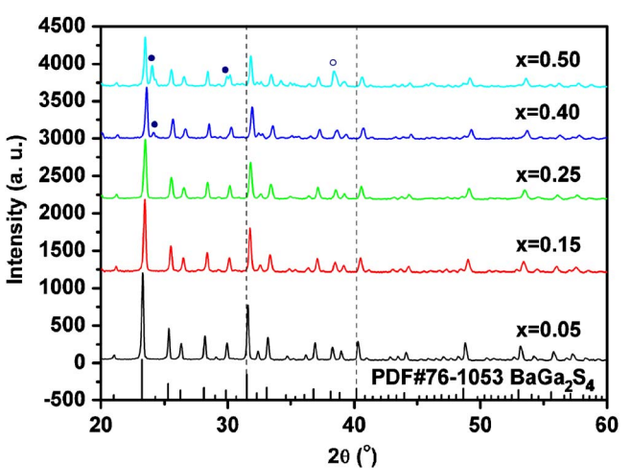

Figure 2. (Color online) XRD patterns of the $Ba_{1-x}Eu_xGa_2S_4$ phosphor samples prepared with various Eu^{2+} ion concentrations. The closed circle indicates the peak of the $EuGa_2S_4$ phase, and the open circle indicates the overlap of the peak of the $EuGa_2S_4$ phase with that of $BaGa_2S_4$ phase.

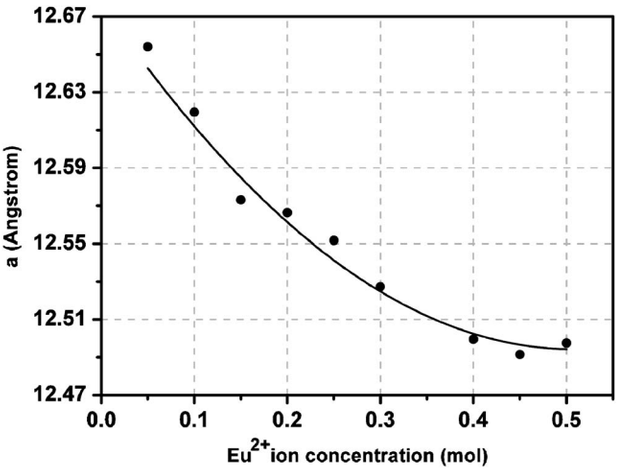

Figure 3. Lattice parameters of the $Ba_{1-x}Eu_xGa_2S_4$ phosphor samples, depending on the Eu^{2+} ion concentration.

of four bands.[12] The band peaking at ~260 nm corresponds to the host lattice absorption. The other bands are assigned to the f-d transitions of Eu^{2+} ions from $4f^7(^8S_{7/2})$ ground state to $4f^6(^7F)5d(e_g)$, $4f^6(^7F)5d(h_g)$, and $4f^6(^7F)5d(t_{2g})$ excited states in the order of increasing wavelength.[12] After deconvolution of the PLE spectrum of each sample into four Gaussian bands, the excitation maximum wavelengths are listed in Table I. The location of the host lattice absorption band was not changed by increase of the Eu^{2+} ion concentration. However, the excitation bands due to the f-d transitions of Eu^{2+} ions were slightly broadened and extended to the longer wavelength with increase of the Eu^{2+} ion concentration.

The redshift of the emission band with increase of the activator concentration is frequently observed in rare-earth-doped phosphors.[14,15] It is often ascribed to the changes of the crystal field strength around the Eu^{2+} ions.[14] As shown in Table I, both the crystal field splitting (CFS) and the Stokes shift were increased with increase of the Eu^{2+} ion concentration. The increase of the CFS was

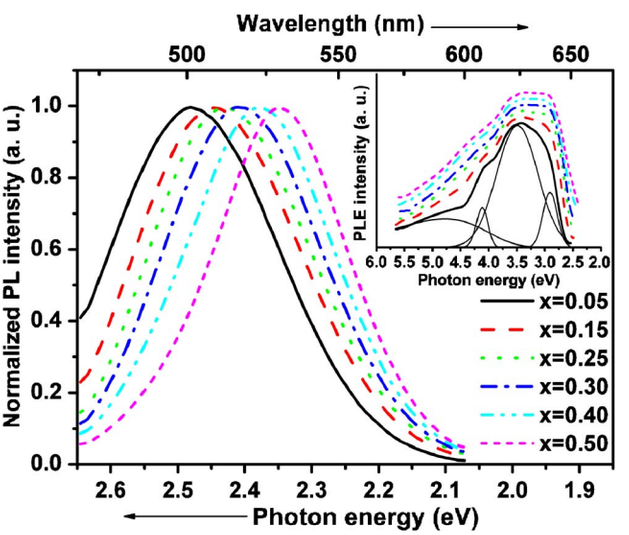

Figure 4. (Color online) Normalized PL spectra of the $Ba_{1-x}Eu_xGa_2S_4$ phosphor samples with various Eu^{2+} ion concentrations ($\lambda_{ex.}$ = 450 nm). The inset shows the normalized PL excitation spectra of the samples with various Eu^{2+} ion concentrations (λ_{em} = the main emission wavelength for each sample).

Table I. Spectral parameters of the $Ba_{1-x}Eu_xGa_2S_4$ phosphor samples.

Eu^{2+} ion concentration (x)	Excitation maximum (nm)				Emission maximum (nm)	Stokes shift (cm^{-1})	CFS (cm^{-1})
	Host lattice	e_g	h_g	t_{2g}			
0.05	260	302	362	429	501	3300	9800
0.15	260	300	359	434	508	3300	10,300
0.25	260	298	364	438	512	3300	10,700
0.30	260	295	361	439	516	3400	11,000
0.40	260	289	359	437	522	3700	11,700
0.50	259	288	356	438	530	3900	11,900

due to the shrinkage of the lattice, when the Ba^{2+} ion is replaced by the smaller Eu^{2+} ion (Fig. 3). The increase of the CFS resulted in increasing the splitting of the 5d levels and lowering of the level from which emission occurs. In addition, the probability of the energy transfers from the higher 5d levels to the lower 5d levels of Eu^{2+} ions increases with increase of the Eu^{2+} ion concentration.[4] It made the emission energy transferred from the excited 5d level to the ground 4f level lower. Therefore, the main emission wavelength was increased with increase of the Eu^{2+} ion concentration. Of course, the contribution of the reabsorption of the high-energy emitted photons due to the overlapping of the emission and excitation spectra cannot be ruled out.[8,12]

Figure 5 shows the relative PL intensity under 450 nm excitation and the main emission wavelength of the $Ba_{1-x}Eu_xGa_2S_4$ phosphor samples prepared with various Eu^{2+} ion concentrations. The PL intensity was increased with increase of the Eu^{2+} ion concentration (x) from 0.05 to 0.25. It was a consequence of the extended excitation bands to the longer wavelength, which could be of great advantage for the white LED applications based on blue emitting LEDs. When the Eu^{2+} ion concentration was >0.3 mol, the PL intensity was decreased with increase of the Eu^{2+} ion concentration. It was thought that the decrease of the PL intensity was mainly due to the nonradiative transitions among the Eu^{2+} ions, which may occur because of exchange interaction, radiation reabsorption, or multipole-multipole interaction.[16,17] The exchange interaction is generally responsible for the energy transfer of forbidden transitions and the typical distance is ~ 5 Å.[16] Because the 4f-5d transition of Eu^{2+} ion was allowed in the BaG_2S_4:Eu^{2+} phosphor and the excitation and emission spectra overlapped, the nonradiative transitions among the Eu^{2+} ions took place due to the electric multipolar interactions or radiation reabsorption. In addition, the formation of the impurity phase $EuGa_2S_4$ could be a possible reason for the decrease of the PL intensity.

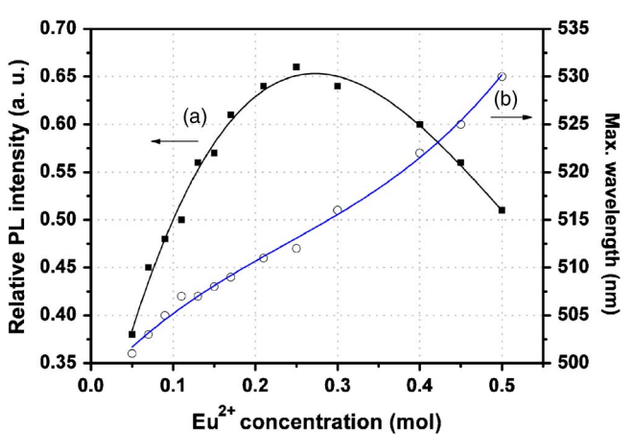

Figure 5. (Color online) Relative PL intensity under 450 nm excitation and the main emission wavelength of the $Ba_{1-x}Eu_xGa_2S_4$ phosphor samples prepared with various Eu^{2+} ion concentrations.

PL properties of $Ba_{1-x-2y}Eu_xCe_yLi_yGa_2S_4$.— In the works of others, it was reported that the energy transfer from Ce^{3+} ion to Eu^{2+} ion enhanced the PL intensity of the Eu^{2+} ion emission in the Eu^{2+} and Ce^{3+} ions codoped phosphors.[18-21] The PLE/PL spectra of $Ba_{0.950}Ce_{0.025}Li_{0.025}Ga_2S_4$ phosphor sample is shown in Fig. 6 with those of the $Ba_{0.95}Eu_{0.05}Ga_2S_4$ phosphor sample. Two bands were observed in the PL spectrum of the $Ba_{0.950}Ce_{0.025}Li_{0.025}Ga_2S_4$ sample, and their separation was due to the energy transitions from the excited 5d level to the ground doublet $^2F_{7/2}$ (493 nm) and $^2F_{5/2}$ (448 nm) levels of the Ce^{3+} ion. The excitation bands at 303 and 390 nm of the $Ba_{0.950}Ce_{0.025}Li_{0.025}Ga_2S_4$ sample were corresponding to the 5d(e_g) and 5d(t_{2g}) bands of Ce^{3+} ion, respectively. As shown in the Fig. 6, the two emission bands of the $Ba_{0.950}Ce_{0.025}Li_{0.025}Ga_2S_4$ phosphor sample were well overlapped with the both the PLE and the PL spectra of the $Ba_{0.95}Eu_{0.05}Ga_2S_4$ sample at the wavelength ranging from 370 to 470 nm and from 450 to 600 nm, respectively. Therefore, it was expected that these spectral overlaps could enhance the PL intensity of the Eu^{2+} ion emission by codoping of the Ce^{3+} ions to $Ba_{1-x}Eu_xGa_2S_4$ phosphor. Figure 7 shows the PLE/PL spectra of the $Ba_{0.95}Eu_{0.05}Ga_2S_4$ phosphor samples with and without the 0.025 mol of Ce^{3+} ion codoping. The

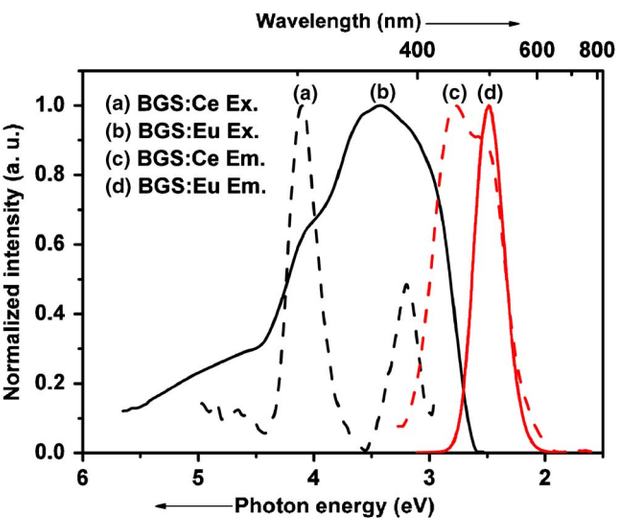

Figure 6. (Color online) PLE/PL spectra of the $Ba_{0.950}Ce_{0.025}Li_{0.025}Ga_2S_4$ (BGS:Ce) and the $Ba_{0.95}Eu_{0.05}Ga_2S_4$ (BGS:Eu) phosphor samples: (a) PLE spectrum of BGS:Ce (λ_{em} = 448 nm), (b) PLE spectrum of BGS:Eu (λ_{em} = 501 nm), (c) PL spectrum of BGS:Ce (λ_{ex} = 303 nm), and (d) PL spectrum of BGS:Eu (λ_{ex} = 364 nm).

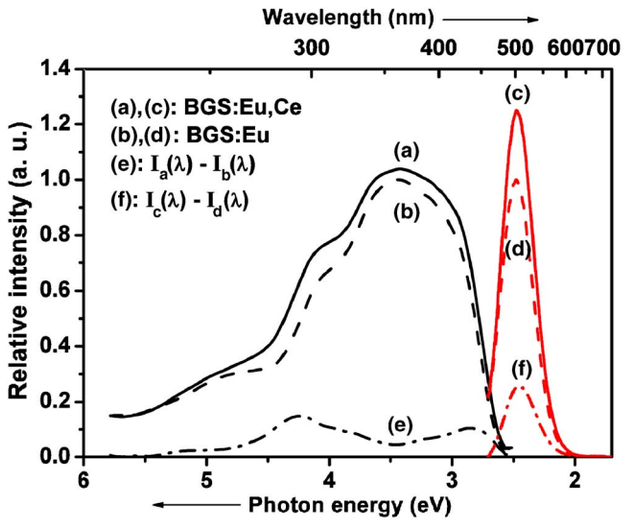

Figure 7. (Color online) PLE/PL spectra of the $Ba_{0.95}Eu_{0.05}Ga_2S_4$ (BGS:Eu) and the $Ba_{0.900}Eu_{0.050}Ce_{0.025}Li_{0.025}Ga_2S_4$ (BGS:Eu, Ce) phosphor samples: (a) PLE spectrum of BGS:Eu, Ce (λ_{em} = 501 nm), (b) PLE spectrum of BGS:Eu (λ_{em} = 501 nm), (c) PL spectrum of BGS:Eu, Ce (λ_{ex} = 450 nm), (d) PL spectrum of BGS:Eu (λ_{ex} = 450 nm), (e) the spectral deviation between (a) and (b), and (f) the spectral deviation between (c) and (d).

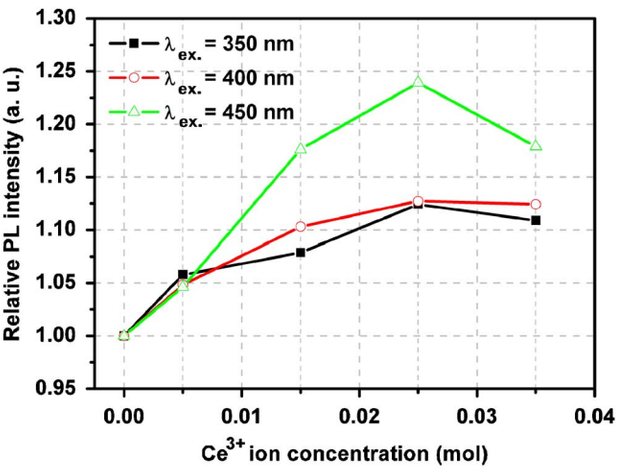

Figure 8. (Color online) Relative PL intensity of Eu^{2+} ion emission of $Ba_{0.95-2y}Eu_{0.05}Ce_yLi_yGa_2S_4$ phosphor samples under the excitation wavelengths of 350, 400, and 450 nm, depending on the concentration of Ce^{3+} ion codoping.

PLE spectra were monitored at the emission wavelength of 501 nm, and the PL spectra were obtained under the excitation wavelength of 450 nm. In the PL spectrum of the $Ba_{0.900}Eu_{0.050}Ce_{0.025}Li_{0.025}Ga_2S_4$ phosphor sample, the Ce^{3+} ion emission was not distinguished and the main emission wavelength was not changed. However, the enhancement of the Eu^{2+} ion emission intensity was observed by codoping of the Ce^{3+} ions. Although there was no Ce^{3+} emission found, in the PLE spectrum of the $Ba_{0.900}Eu_{0.050}Ce_{0.025}Li_{0.025}Ga_2S_4$ phosphor sample, some spectral deviation from that of the $Ba_{0.95}Eu_{0.05}Ga_2S_4$ phosphor sample was observed. Curve (e) in Fig. 7 shows the spectral deviation, which matched well with the PLE/PL spectra of the $Ba_{0.950}Ce_{0.025}Li_{0.025}Ga_2S_4$ phosphor sample (Fig. 6). That meant that the energy absorbed by the Ce^{3+} ions was transferred to the Eu^{2+} ions. For the dipole-dipole interaction, the energy transfer rate from Ce^{3+} ion to Eu^{2+} ion was about 10^9–10^{10} s^{-1}, which was one to two orders of magnitude higher than that of Ce^{3+} ion emission transition (10^8 s^{-1}) from the excited 5d level to the ground 4f levels.[19] Therefore, the energy absorbed by Ce^{3+} ions was more likely transferred to the Eu^{2+} ions and enhanced the PL intensity of the Eu^{2+} ion emission than showed the Ce^{3+} ion emission.

Sensitizing with the Ce^{3+} ion enhanced the PL intensity of the Eu^{2+} ion emission under the various excitation wavelengths ranging from near ultraviolet (UV) to blue. Figure 8 shows the relative PL intensity of Eu^{2+} ion emission of $Ba_{0.95-2y}Eu_{0.05}Ce_yLi_yGa_2S_4$ phosphor samples under the excitation wavelengths of 350, 400, and 450 nm, depending on the concentration of Ce^{3+} ion codoping. The PL intensity of the $Ba_{0.900}Eu_{0.050}Ce_{0.025}Li_{0.025}Ga_2S_4$ phosphor sample was higher by 24% than that of the $Ba_{0.95}Eu_{0.05}Ga_2S_4$ phosphor sample under 450 nm excitation.

CIE chromaticity coordinates.— Figure 9 shows the Commission International de l'Eclairge (CIE) 1931 chromaticity coordinates of the $Ba_{1-x}Eu_xGa_2S_4$ phosphor samples prepared with various Eu^{2+} ion concentration. The $Ba_{0.95}Eu_{0.05}Ga_2S_4$ phosphor sample showed bluish-green emission (x = 0.143, y = 0.506). The chromaticity coordinates were largely shifted to the green emission region just by changing the Eu^{2+} ion concentration, and the chromaticity coordinate of the $Ba_{0.50}Eu_{0.50}Ga_2S_4$ phosphor sample was (x = 2.414, y = 0.658). Because the main emission wavelengths of the phosphor samples were not changed by codoping of Ce^{3+} ions, the chromaticity coordinates of the $Ba_{0.95-2y}Eu_{0.05}Ce_yLi_yGa_2S_4$ phosphor samples were almost the same as those of the $Ba_{0.95}Eu_{0.05}Ga_2S_4$ phosphor sample. Comparing to the three band white LED, which was made by combining a blue emitting InGaN-based LED chip with commercial sulfide red/green phosphors, such as $CaS:Eu^{2+}$ and $SrGa_2S_4:Eu^{2+}$, the four band white LED could extend their color gamut by adding of the $BaGa_2S_4:Eu^{2+}$ phosphor. Therefore, it is believed that one could easily design the chromaticity coordinates, the color temperature, and the CRI value of the white LEDs by adopting and controlling of the $BaGa_2S_4:Eu^{2+}$, Ce^{3+} phosphor.

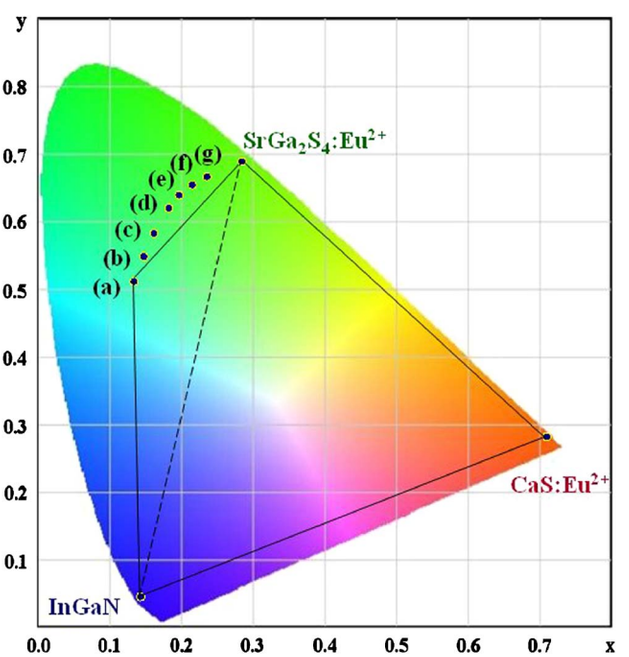

Figure 9. (Color online) CIE chromaticity coordinates of the $Ba_{1-x}Eu_xGa_2S_4$ phosphor samples prepared with various Eu^{2+} ion concentrations of (a) 0.05, (b) 0.10, (c) 0.15, (d) 0.25, (e) 0.30, (f) 0.40, and (g) 0.50. The CIE chromaticity coordinates of the InGaN-based LEDs (blue), $SrGa_2S_4:Eu^{2+}$ phosphor (green), and $CaS:Eu^{2+}$ phosphor (red) were included.

Conclusion

$Ba_{1-x-2y}Eu_xCe_yLi_yGa_2S_4:Eu^{2+}$ phosphor samples were synthesized by a solid-state reaction method. Because the ionic radius of Eu^{2+} ion was smaller than that of the Ba^{2+} ion, the lattice parameter of the samples was decreased with increase of the Eu^{2+} ion concentration. PL properties of $Ba_{1-x}Eu_xGa_2S_4$ phosphor was severely varied depending on the Eu^{2+} ion concentration. The main emission wavelength was moved from 501 to 530 nm with increase of the Eu^{2+} ion concentration (x) from 0.05 to 0.50. The redshift of the emission band was due to the increase of the CFS. The increase of the CFS resulted in increasing the splitting of the 5d levels and lowering of the level from which emission occurs, and thus the emission band was shifted to the longer wavelengths. The relative PL intensity under 450 nm excitation was increased with increase of the Eu^{2+} ion concentration (x) from 0.05 to 0.25 due to the extended excitation band to the longer wavelengths. However, when the Eu^{2+} ion concentration $x > 0.3$, the relative PL intensity was decreased due to the nonradiative transitions among the Eu^{2+} ions and the formation of $EuGa_2S_4$ impurity phase. Ce^{3+} ion codoping enhanced the PL intensity of the Eu^{2+} ion emission under near UV and blue excitation due to the energy transfer from Ce^{3+} ion to Eu^{2+} ion. The PL intensity of the $Ba_{0.900}Eu_{0.050}Ce_{0.025}Li_{0.025}Ga_2S_4$ phosphor sample was higher by 24% than that of the $Ba_{0.95}Eu_{0.05}Ga_2S_4$ phosphor sample under 450 nm excitation. The CIE chromaticity coordinates were largely shifted from the bluish-green emitting region ($x = 0.143$, $y = 0.506$) to green emitting one ($x = 2.414$, $y = 0.658$) with increase of Eu^{2+} ion concentration (x) from 0.05 to 0.50.

The Components and Materials Technology Development Program funded by the Ministry of Commerce, Industry and Energy of the Korean government assisted in meeting the publication costs of this article.

References

1. S. Nakamura and G. Fasol, *The Blue Laser Diode: GaN Based Light Emitters and Lasers*, Springer, Berlin (1997).
2. J. K. Park, M. A. Lim, C. H. Kim, H. D. Park, J. T. Park, and S. Y. Choi, *Appl. Phys. Lett.*, **82**, 683 (2003).
3. M. P. Saradhi and U. V. Varadaraju, *Chem. Mater.*, **18**, 5267 (2006).
4. R.-J. Xie, N. Hirosaki, K. Sakuma, Y. Yamamoto, and M. Mitomo, *Appl. Phys. Lett.*, **84**, 5404 (2004).
5. Y. Q. Li, A. C. A. Delsing, G. de With, and H. T. Hintzen, *Chem. Mater.*, **17**, 3242 (2005).
6. N. Hirosaki, R.-J. Xie, K. Kimoto, T. Sekiguchi, Y. Yamamoto, T. Suehiro, and M. Mitomo, *Appl. Phys. Lett.*, **86**, 211905 (2005).
7. K. Uheda, N. Hirosaki, Y. Yamamoto, A. Naito, T. Nakajima, and H. Yamamoto, *Electrochem. Solid-State Lett.*, **9**, H22 (2006).
8. R.-J. Xie, N. Hirosaki, T. Suehiro, F.-F. Xu, and M. Mitomo, *Chem. Mater.*, **18**, 5578 (2006).
9. Y.-D. Huh, J.-H. Shim, Y. Kim, and Y. R. Do, *J. Electrochem. Soc.*, **150**, H57 (2003).
10. N. Kimura, K. Sakuma, S. Hirafune, K. Asano, N. Hirosaki, and R.-J. Xie, *Appl. Phys. Lett.*, **90**, 051109 (2007).
11. T. E. Peters and J. A. Baglio, *J. Electrochem. Soc.*, **119**, 230 (1972).
12. R. B. Jabbarov, C. Chartier, B. G. Tagiev, O. B. Tagiev, N. N. Musayeva, C. Barthou, and P. Benalloul, *J. Phys. Chem. Solids*, **66**, 1049 (2005).
13. M. R. Davolos, A. Garcia, C. Fouassier, and P. Hagenmuller, *J. Solid State Chem.*, **83**, 316 (1989).
14. G. Blasse and B. C. Grabmaier, *Luminescence Materials*, Springer-Verlag, Berlin (1994).
15. Y. Q. Li, G. de With, and H. T. Hintzen, *J. Alloys Compd.*, **385**, 1 (2004).
16. L. G. Van Uitert, *J. Electrochem. Soc.*, **114**, 1048 (1967).
17. D. L. Dexter, *J. Chem. Phys.*, **21**, 836 (1953).
18. W. Lehman and F. M. Ryan, *J. Electrochem. Soc.*, **118**, 477 (1971).
19. D. Jia, *J. Electrochem. Soc.*, **153**, H198 (2006).
20. V. Sivakumar and U. V. Varadaraju, *J. Electrochem. Soc.*, **154**, J167 (2007).
21. R. B. Dzhabbarov, *Semiconductors*, **36**, 394 (2002).